JAERI-M
9647

CREEP TEST OF TYPE 304 STAINLESS STEEL CYLINDRICAL TUBE SUBJECTED TO INTERNAL PRESSURE

August 1981

Shuzo UEDA, Ryoichi KURIHARA
and Toshihiro OBA

日本原子力研究所
Japan Atomic Energy Research Institute

この報告書は，日本原子力研究所がJAERI-Mレポートとして，不定期に刊行している研究報告書です．入手，複製などのお問合わせは，日本原子力研究所技術情報部（茨城県那珂郡東海村）あて，お申しこしください．

JAERI-M reports, issued irregularly, describe the results of research works carried out in JAERI. Inquiries about the availability of reports and their reproduction should be addressed to Division of Technical Information, Japan Atomic Energy Research Institute, Tokai-mura, Naka-gun, Ibaraki-ken, Japan.

JAERI-M 9647

Creep Test of Type 304 Stainless Steel Cylindrical Tube Subjected to Internal Pressure

Shuzo UEDA, Ryoichi KURIHARA and Toshihiro OBA

Division of Reactor Safety,
Tokai Research Establishment, JAERI

(Received August 6, 1981)

This report summarizes results of experimental creep tests of type 304 stainless steel tube subjected to internal pressure at 650°C. The test equipment was developed for these tests.

The smooth tubes were tested at pressures of 9.32 and 7.36 MPa. Test results indicate that the rupture time of tubes is in good agreement with that of uniaxial specimens when the maximum stress or the equivalent stress is taken as the rupture criterion. The tubes containing axial and circumferential surface notches were tested at the pressure of 7.36 MPa. Test results indicate that the ductile fracture theory is applicable, to some extent, to the life prediction for case of axial notches but not applicable for case of circumferential notches.

An electric potential method was very useful for monitoring the creep crack growth from the notch tip. The relationship between the creep crack growth rate and the fracture mechanics parameter σ_{net} or K_I was investigated.

Keywords; Creep, Notch, Creep Rupture, Creep Crack, Crack Growth Rate, Creep Elongation, 304 Stainless Steel, Cylindrical Tube, Pressure Dependence

JAERI-M 9647

内圧を受ける304ステンレス鋼製円筒容器のクリープ試験

日本原子力研究所東海研究所安全工学部
植田　脩三・栗原　良一・大場　敏弘

（1981年8月6日受理）

内圧クリープ試験装置を製作し，高温で使用される圧力容器と配管を模擬した平滑および切欠付SUS304ステンレス鋼製円筒について650℃の温度でクリープ試験をおこなった。

平滑試験体については，9.32 MPa，7.36 MPaの圧力でクリープ破断試験をおこない破断寿命は等価応力（σ_{eq}）または最大応力のクリープ破断基準を取ることにより単軸のクリープ破断寿命と一致することが確かめられた。

切欠試験体については軸方向，周方向の各種の表面切欠についてのクリープ破断試験をおこない寿命の低下を測定した。寿命の予測に際して延性破断の式を適用することは軸方向切欠の場合は良いが，周方向切欠では無理であることが判明した。

切欠先端からのクリープの成長のモニタリングには電気ポテンシアル法が有効であることが示唆された。

実験から得られたクリープき裂成長速度を破壊力学パラメータであるK値やσ_{net}で整理することを試みた。

Contents

目　　次

I. INRTODUCTION

Research on the creep rupture of the cylindrical tube containing a notch subjected to internal pressure is concerned to the integrity of fuel claddings, steam generator tubes or pipings. This research has been done from two standpoints of view, namely the effects of notches on creep rupture and creep crack growth.

King[1], Gest and Hutching[2] studied the creep strength of fuel claddings or steam generator tubes with axial surface notches. They find that the notch effect can be calculated from the ductile fracture equation of the cylindrical tube proposed by Hahn[3].

On the other hand To and Chopra studied this problem from the standpoints of the creep crack growth and tried to apply the fracture mechanics to this problem.

Chopra used the stress intensity factor K_I to correlate the creep crack growth rate with the shape of notch and loading[4].

The authors performed the experiments on cylindrical tubes which were 100 mm in inner diameter, 3 mm in thickness and 540 mm in length, at 650°c. The material is type 304 stainless steel which will be used as one of structural materials in the construction of the Japanese experimental VHTR and related experimental facilities.

In these experiments the axial and circumferential surface notches of various lengths were machined on the outer surface of tubes. Creep crack growth from the notch tip was monitored by an electric potential method. The effect of notches on the creep strength and the creep crack growth rate was investigated.

2. EXPERIMENTAL METHOD

2.1 Equipment

The schematic of the test equipment is shown in Fig.1. This equipment was developed for the creep test on piping components loaded by constant or cyclic internal pressure at high temperatures. The pressure medium is Argon gas which is supplied from the commercial gas tank. Test pressures are controlled by a semi-automatic regulator valve. Pressure cycling rate is performed using an electric magnetic valve. Holding time is controlled by timers. Test tubes were heated in the electric furnace.

The temperature along the axis of the test tube was 650±3°C within ±80 mm from the centre of test tube. Diametral creep deformations were measured at three locations as shown in Fig.1. Six quarts glass rods were inserted from the outer surface of the furnace. Three sets of displacement transducers were installed at the tips of quarts rods in order to measure the creep deformation. The creep deformation was recorded continuously by multi-penrecorders. The diametral creep deformation is twice of the average radial creep deformation.

2.2 Test Tubes and Test Conditions

The shape of test tubes is shown in Fig.2. The test tube is 100 mm in inner diameter, 3 mm in thickness and 540 mm in total length. The test section of the tube is 270 mm in length. A steel core was confined in the test tube to reduce the gas volume. Artificial surface notches were machined on the outer surface of the test tubes in the axial and circumferential directions. The axial notch was machined by the electric discharing method. The axial notch was 13, 25, 100 and 150 mm in length and 0.5, 1.0 and 1.3 mm in depth respectively.

The circumferential notch was machined by the cutter so that the angle of notch was 60 degrees and the radius of the notch root was 0.3 mm. The circumferential notch was 1.0 mm in depth, $\pi D/4$, $\pi D/2$, $3\pi D/4$ and πD in length respectively.

The cylindrical tube without the notch was tested at several different pressure levels at 650°C.

The cylindrical tubes with various notches were tested at 7.35 MPa, (75 kg/cm^2) at 650°C.

2.3 Electric Potential Method for Creep Crack Growth Measurement.

The electric potential method was used to measure the creep crack growth from the notch tip. The arrangement of electric potential probes at the notch is illustrated in Fig.3. Probes were made of type 304 stainless steel welding rods of 1.0 mm in diameter. They were welded at the center of notches at the intervals of 3 mm. The value of the constant electric current used in those experiments was five amperes. The variation of electric potential between inner two probes was monitored.

A calibration curve is needed to transform the output voltage to the crack growth. The calibration curve was made by using type 304 stainless steel plate with artificial notches of known dimensions and measuring electric potentials under the same conditions as test tubes. The shape of notch was assumed to be elliptic. The calibration curve is shown in Fig.4.

2.4 Creep Characteristics Of Test Materials

Test material is the forging of the type 304 stainless steel. This material is the same one which is used in the research on the structural strength of members used at high temperatures performed by the first subcommittee 11G, Technical Research Association for Integrity of Structures at Elevated Service Temperatures. Brief summary of the results of material tests performed in that committee is described in this paragraph.[5] Mechanical properties of this material are shown in Tables 1 and 2.

The creep deformation behavior of test materials is shown in Figs.5 and 6. The minimum creep rate $\dot{\varepsilon}_{min}$ is calculated from these curve and the relation between $\dot{\varepsilon}_{min}$ and the stress is plotted on the logarithmic graph as shown in Fig.7. The good relationship is obtained as the following equation.

$$\log \sigma_r = 0.123 \log \dot{\varepsilon}_{min} + 1.54 \qquad (1)$$

The constitutive equation used for steady state creep analysis is given by the next equation for this material.

$$\varepsilon = 3.02 \times 10^{-13} \sigma_r^{8.13} t \qquad (2)$$

The duration of transient creep is about several ten hours.

The creep rupture time, t_r and the creep elongation versus time are

plotted in Figs.8 and 9. The relation between the rupture stress and the rupture time is given by the following equation.

$$\log \sigma_r = -0.14 \log t_r + 2.49 \tag{3}$$

In addition the minimum creep rate $\dot{\varepsilon}_{min}$ has a good relationship with the rupture stress, given by

$$\log \dot{\varepsilon}_{min} = -1.16 \log t_r - 0.157 \tag{4}$$

The initiation time of tertiary creep is considered as the time of crack initiation. The ratio of the initiation time of tertiary creep to the creep rupture time is given by the following equation.

$$t_{r^3} = 0.569\ t_r^{0.947} \tag{5}$$

3. Test Results

3.1 Creep Deformation

Test reults are summarized in table 3. The creep rupture time t_r, the minmum creep rate $\dot{\varepsilon}_{min}$ and the average creep rupture strain ε_c are shown in this table. The average creep strain ε_c was calculated from the following equation.

$$\varepsilon_c = \left[\left(\frac{D_1^2 + D_2^2}{2D^2} \right)^{\frac{1}{2}} - 1 \right] \times 100 \qquad (6)$$

where D : Outer diameter of tube before test

D_1: Outer diameter of tube at ruptured section after test

D_2: Outer diameter of tube in the vertical direction to diameter after test

The value of average creep rupture strain ε_c ranges from 7.7 to 24.7%. The value of the average creep rupture strain of tube at stess level, 127MPa is about half of that of the uniaxial test specimen. The average creep rupture strain is reduced by the presence of notches. An example of the residual creep deformation is shown in Fig.10 for case of the axial notch. The residual creep deformation of notched tube is smaller than that of the smooth tube and a local bulging is caused around the notch in the notched tube. An example of the residual creep deformaion is shown in Fig.11 for case of the circumferential notch. The difference between the residual creep deformations of two tubes is small although one of tubes has the notch of 1 mm depth. The local bulging is not caused in this case. A restriction against the creep deformation is rather caused in circumferentially notched tubes.

The time history of the diametral creep deformation at the centre of the tubes with and without axial notches is shown in Fig.12. The diametral creep deformations are plotted on the same curve until twenty hours and thereafter are apart each other from this curve because of the local bulging. The longer the initial notch is, the earlier the deviation of the creep curve of the notched specimen and the smaller the creep strain at the rupture.

3.2 Creep Rupture Time

The rupture time of test tubes is shown in Fig.13. It is clear that the creep rupture time is reduced by the surface notch. The relation between the creep rupture time, t_r and the strees σ_r, for the smooth tubes is given by the following equations.

$$\log \sigma_{\theta,r} = -0.136 \log t_r + 2.50 \quad (7)$$

$$\log \sigma_{eq,r} = -0.136 \log t_r + 2.45 \quad (8)$$

This equation was determined by a least square method. Some data were obtained in the labaratoy of Japan Steel Works Co.[5] The relation between the rupture stress σ_r and the rupture time t_r for the uniaxial specimens is described by

$$\log \sigma_r = -0.14 \log t_r + 2.51 \quad (9)$$

From these experiments the maximum principal stress or the equivalent stress is good as the criterion of creep rupture under the biaxial stress state. King, Gest and Hutching adopted the ductile fracture theory for evaluating the creep strength reduction in thier tests concerning fuel claddings (SUS 316) and boiler tubes (9% Cr - 1% Mo steel) for case of the axial notches.

In this theory it is considered that the fracture is caused when the flow stress of the notched section attains the creep rupture stress.

The ductile fracture equations are as follows.

(1) Axial notch (Hahn's equation)

The strength reduction ratio is given by

$$\frac{\sigma_{r,d}}{\sigma_{r,d}} = \frac{h/d-1}{h/d-1/M} \quad (10)$$

$M = (1 + 1.16\ c^2/Rh)$

d---- Depth of crack

c---- Half of crack length

R---- Mean radius of test tube

h---- Thickness of test tube

M---- Folias stress magnification factor

(2) Circumferential Notch

Flow stress at the notched section is given by

$$\sigma_{flow} = \frac{Pr}{2h} + \frac{Y\pi R_i^2 p}{Z} \quad (11)$$

Where

R_i : Inner radius of test tube

Y : Moment arm of cracked section

Z : Sectional modulus of these specimens at notched section

In Table 3 the experimental creep strength reduction ratio and the creep strength ratio based on Hahn's equation are described. The experimental creep strength reduction ratio is slighty smaller than the theoretical one in all the experiments.

In the circumferential notches, the flow stresses calculated from equation(11) are less than the nominal circumferential stress, 126 MPa as shown in Table 4. It is clear that the flow stress equation is not useful for the explanation of the rupture for case of the circumferential notches. However this table indicates that the flow stress for partial circumferential notch is higher than that for the full cirumferential notch, and the creep life of tube with the partial circumferential notch may be shorter than that of the tube with the full circumferential notch. Actually this phenomenon is occured as shown in Fig.14. In Fig.15 is shown the creep strength reduction ratio versus the surface shell parameter $\frac{c}{\sqrt{Rh}}$ $(\frac{d}{h})$ [6] for case of axial notches. There seems to be a good relationship between them.

3.3 Creep Crack Growth

In paragrapf 3.2, the creep life prediction was done on the basis of the idea that the tube breaks instantaneously when the loading time attains the creep rupture time t_r. Actually the crack initiates at the notch root in the early stage of the creep life and grow to through the thickness. Therefore if the creep crack growth rate is measured and correlated to the fracture mechanics parameter, the creep life prediction will be done more precisely. Such investigation were tried by To[7] and Chopra. Although this trial cannot be expected to be precise in the state of the art, the authors also tried to correlate the creep crack growth rate with the net section stress or the stress intensity factor. The creep crack growth curve is shown in Fig.16. These curves were obtained by calculating the creep crack growth from the output voltage of the electric potential probes using the calibration curve shown in Fig.4

These creep crack growth curves were approximated by a polynomial equation by the least square method. The creep crack growth rate was calculated from this polynomial equation by the differentiation.

The net section stress σ_{net} and the stress intensity factor K_I are calculated by the next equations

(1) Axial crack

a) The net section stress is given by

$$\sigma_{net} = \frac{2ch}{2ch - [2cd + \pi c(a-d)/2]} \cdot \frac{PR}{h} \qquad (12)$$

b) The stress intensity factor is given by[8]

$$K_I = [1 + 0.12(1 - \frac{a}{c})]\frac{\sqrt{(\pi a)^{1/2}}}{\phi}\left\{\frac{2h}{\pi a}\tan\frac{\pi a}{2h}\right\}^{1/2} \quad (13)$$

$$\Phi = \int_0^{\frac{\pi}{2}}[1 - (\frac{a^2}{c^2})\sin^2\phi]^{1/2}d\phi$$

(2) Circumferential notch

a) The net section stress is given by

$$\sigma_{net} = \frac{PR}{2h}\cdot\frac{h}{h-a} \quad (14)$$

b) The stress intensity facter is given by

$$\frac{K_I}{K_0} = \frac{1-N^2}{(1-(1-N)X)^2-N^2}\left\{0.80 + \frac{(1-N)X}{1-(1-N)X}\left[4 + \frac{1.08N}{(1-N)(1-x)}\right]\right\}^{1/2} \quad (15)$$

where

$N = R_I/R_O$ and $X = a/(R_O - R_I)$

Ko is given by

$Ko = \sigma\sqrt{\pi a}$

In the axial crack, the effect of the shell curvature is neglected when calculating these quantities. In the circumferential crack, only the axial force due to internal pressure is considered.

The relation between the creep crack growth rate $\frac{da}{dt}$ and the net section stess σ_{net} is shown in Fig.17. There is a linear relationship between the both on the logarithmic graph for each experimental case respectively.

The relatianohip between the creep crack growth rate $\frac{da}{dt}$ and the stess intensity factor K_I is shown in Fig.18. There is also a good relationship between the both quantities. From these two figures, it is difficult to say which parameter is better for characterizing the creep crack growth rate. For the axial crack, the gradient of the correlation is different for each crack length. This seems to be that the bending effect due to the local bulging around the surface notch is neglected when calulating the fracture mechanics parameters.

4. Fracture Appearance

Fracture appearances of test tubes are shown in Fig.19 for case of the axial notch. When the initial notch length is larger, the opening area is larger. Ductile fracture occured in the experiments of long initial notches of 100 and 150mm.

Fracture appearances of test tubes are shown in Fig.20 for case of the circumferential notch. Cracks only grew in the direction of the thickness in all the experiments.

b) The stress intensity factor is given by[8]

$$K_I = [1 + 0.12(1 - \frac{a}{c})]\frac{\sigma(\pi a)^{1/2}}{\Phi}\left\{\frac{2h}{\pi a}\tan\frac{\pi a}{2h}\right\}^{\frac{1}{2}} \quad (13)$$

$$\Phi = \int_0^{\frac{\pi}{2}}[1 - (\frac{a^2}{c^2})\sin^2\phi]^{\frac{1}{2}}d\phi$$

(2) Circumferential notch

a) The net section stress is given by

$$\sigma_{net} = \frac{PR}{2h}\cdot\frac{h}{h-a} \quad (14)$$

b) The stress intensity facter is given by

$$\frac{K_I}{K_0} = \frac{1-N^2}{(1-(1-N)X)^2-N^2}\left\{0.80 + \frac{(1-N)X}{1-(1-N)X}\left[4 + \frac{1.08N}{(1-N)(1-x)}\right]\right\}^{\frac{1}{2}} \quad (15)$$

where

$N = R_I/R_O$ and $X = a/(R_O - R_I)$

Ko is given by

$Ko = \sigma\sqrt{\pi a}$

In the axial crack, the effect of the shell curvature is neglected when calculating these quantities. In the circumferential crack, only the axial force due to internal pressure is considered.

The relation between the creep crack growth rate $\frac{da}{dt}$ and the net section stess σ_{net} is shown in Fig.17. There is a linear relationship between the both on the logarithmic graph for each experimental case respectively.

The relatianohip between the creep crack growth rate $\frac{da}{dt}$ and the stess intensity factor K_I is shown in Fig.18. There is also a good relationship between the both quantities. From these two figures, it is difficult to say which parameter is better for characterizing the creep crack growth rate. For the axial crack, the gradient of the correlation is different for each crack length. This seems to be that the bending effect due to the local bulging around the surface notch is neglected when calulating the fracture mechanics parameters.

4. Fracture Appearance

Fracture appearances of test tubes are shown in Fig.19 for case of the axial notch. When the initial notch length is larger, the opening area is larger. Ductile fracture occured in the experiments of long initial notches of 100 and 150mm.

Fracture appearances of test tubes are shown in Fig.20 for case of the circumferential notch. Cracks only grew in the direction of the thickness in all the experiments.

5. Concluding Remarks

The creep strength reduction of the type 304 stainless steel cylindrical tube containing the axial or circumferential surface notch was investigated at 650°C under the internal pressure. The following conclusions are obtained.

(1) When the surface notches are axial, the creep strength reduction ratio can be predicted to some extent by the ductile fracture theory proposed by Hahn. However the experimental creep strength reduction ratio is 10% lower than that ratio based on the ductile fracture theory. When the surface notches are circumferential the creep strength reduction ratio cannot be predicted by the ductile fracture theory.

(2) There seems to be a good relationship between the experimental creep strength reduction ratio for case of the axial notches and the surface shell parameter, $\frac{c}{\sqrt{Rh}}$ $(\frac{d}{h})$, as far as experimental results are concerned.

(3) Cracks only grow from the notch tip to the thickness direction in all the experiments.

(4) The electric potential method is very useful to measure the creep crack growth from the notch tip.

(5) The relation between the creep crack growth rate and the fracture mechanics parameters. σ_{net} or K_I is linear on the logarithmic graph. It is difficult to say which parameter is better for correlating the creep crack growth rate.

Acknowledgement

The authors would like to thanks Dr. Miyazono, chief of Mechanical Strength and Structure Laboratory, Japan Atomic Energy Research Institute for his useful comments on this research. The authors would appreciate Dr. Fujimura, Technical Research Association for Integrity of Structures at Elevated Service Temperatures for his great support.

5. Concluding Remarks

The creep strength reduction of the type 304 stainless steel cylindrical tube containing the axial or circumferential surface notch was investigated at 650°C under the internal pressure. The following conclusions are obtained.

(1) When the surface notches are axial, the creep strength reduction ratio can be predicted to some extent by the ductile fracture theory proposed by Hahn. However the experimental creep strength reduction ratio is 10% lower than that ratio based on the ductile fracture theory. When the surface notches are circumferential the creep strength reduction ratio cannot be predicted by the ductile fracture theory.

(2) There seems to be a good relationship between the experimental creep strength reduction ratio for case of the axial notches and the surface shell parameter, $\frac{c}{\sqrt{Rh}}$ $(\frac{d}{h})$, as far as experimental results are concerned.

(3) Cracks only grow from the notch tip to the thickness direction in all the experiments.

(4) The electric potential method is very useful to measure the creep crack growth from the notch tip.

(5) The relation between the creep crack growth rate and the fracture mechanics parameters. σ_{net} or K_I is linear on the logarithmic graph. It is difficult to say which parameter is better for correlating the creep crack growth rate.

Acknowledgement

The authors would like to thanks Dr. Miyazono, chief of Mechanical Strength and Structure Laboratory, Japan Atomic Energy Research Institute for his useful comments on this research. The authors would appreciate Dr. Fujimura, Technical Research Association for Integrity of Structures at Elevated Service Temperatures for his great support.

References

(1) King, R. T., Cook, K. V. & Reimann G. A. 'Biaxial Creep-Rupture Properties of Defective Stainless Steel Tubing', ORNL-TM-3711

(2) Guest, J. C. & Hutching, J. A. 'Pressure Tests to Assess The Significance of Defects in Boiler and Superheater Tubing', International Conference on creep and fatigue in elevated temperature applications, Conference Publication 13

(3) Hahn, G. T., Sarrat, M. & Rosenfield, A. R. 'Criterion for Crack Extension in Cylindrical Pressure Vessels', Int. Jnl. Fract. Mech. 1969, 5, 187.

(4) CHOPRA, P. S. 'Finite Element Fracture Mechanics Analysis of Creep Rupture of Fuel Element Cladding' Proceedings of 2nd International Conference on Structural Mechanics in Reactor Technology, 1973, C2/5.

(5) First Subcommittee, 1/G, 'Structural Strength of Members used at High Temperatures and Its Application to Structural Design', ISES 7712, 1977, Dec.

(6) J. C. Newman ' Fracture Analysis of Surface and Through Cracks in Cylindrical Pressure Vessels,' NASA TN D08325, 1976.

(7) To, K. C. 'A Phenominological Theory of Subcritical Creep Critical Crack Growth In A Cylindrical Vessel Weakend By An Axial Part-through Crack', Int. J. Pres. & Piping, (4), 1976, P.63.

(8) Paris, P. C. and Shih, C. F. 'Stress Analysis of Cracks', ASTM STP No.381, 1965, P.30.

Table 1 Mechanical Properties of Material at Room Temperature

0.2% Proof Stress (MPa)	Ultimate Strength (MPa)	Elongation (%)	Reduction of Area. (%)	Hardness (H_B)
261	569	65.0	76.2	148

Table 2 Mechanical Properties of Material at 650 °C

Strain Rate at Proof Stress %/min	0.2% Proof Stress (MPa)	Ultimate Strength (MPa)	Elongation (%)	Reduction of Area (%)
0.05	146	312	47.5	73.0
0.50	121	312	47.9	76.9

Table 4 Flow Stress of Test Tube with Circumferential Notch

θ	Shift of Centroid (mm)	Moment of Inertia mm^4	Bending Stress MPa	Flow Stress MPa
0	0	1.29×10^6	0	63.3
90°	4.4	1.12×10^6	7.55	102
180°	6.8	1.10×10^6	21.2	116
270°	5.4	1.04×10^6	17.2	112
360°	0	8.33×10^5	0	95.0

Table 3 Summary of Test Conditions and Results

Specimen No.	Test Pressure (MPa)	Nominal Circumferential Stress (MPa)	Notch Length (mm)	Notch Depth (mm)	Rupture Time (Hr)	Average Creep Rupture Strain (%)	Minimum Creep Rate (1/Hr)	σ_θ, notch / σ_θ, smooth	
								Experiment	Ductile Fracture Theory
1	9.32	160	0	0	108	—	8.0×10^{-4}	1.0	1.0
2	7.36	127	0	0	825	24.7	1.09×10^{-4}	1.0	1.0
3	7.36	127	Longitudinal 5	1.0	371	13.0	1.04×10^{-4}	0.803	0.985
4	7.36	127	Longitudinal 25	1.0	112	7.7	1.11×10^{-4}	0.751	0.839
5	7.36	127	Longitudinal 50	1.0	69	7.4	1.24×10^{-4}	0.703	0.759
6	7.36	127	Longitudinal 100	1.0	29	11.9	—	0.624	0.712
7	7.36	127	Longitudinal 13	1.3	186	8.9	1.10×10^{-4}	0.804	0.886
8	7.36	127	Longitudinal 150	1.3	12	15.0	—	0.554	0.601
9	7.36	127	Longitudinal 25	0.5	230	—	—	0.827	0.929
10	7.36	127	All Periphery	1.0	560	22.6	—	0.934	*
11	7.36	127	3/4 Periphery	1.0	507	14.6	—	0.921	*
12	7.36	127	Half Periphery	1.0	489	12.8	—	0.917	*
13	7.36	127	Quarter Periphery	1.0	486	16.4	—	0.916	*

* See Table 4

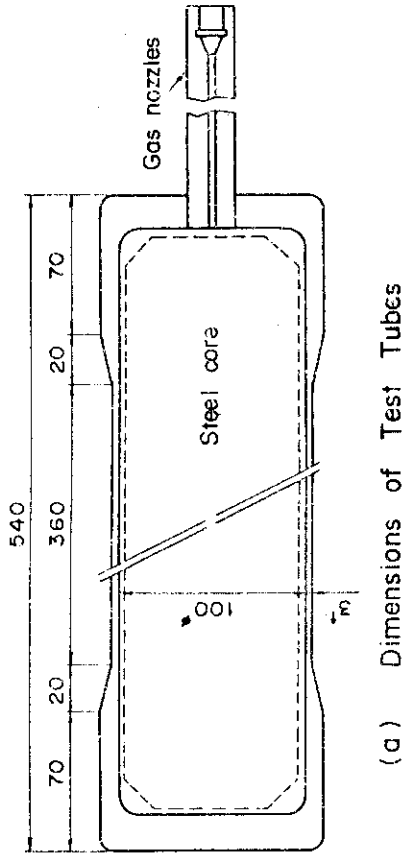

(a) Dimensions of Test Tubes

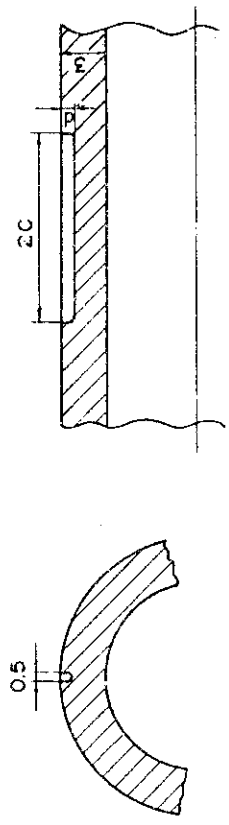

(b) Shape of Axial Notch

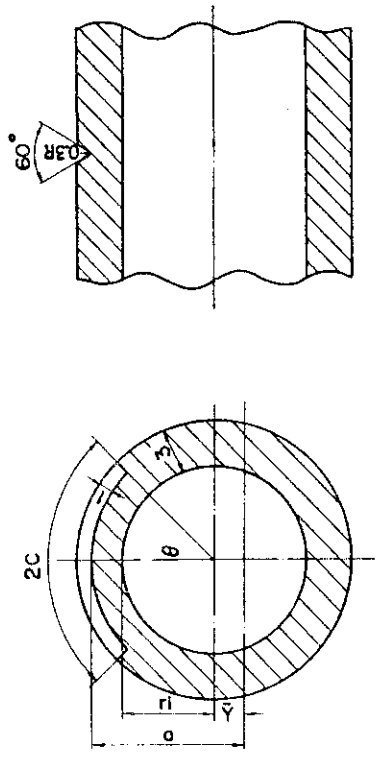

(c) Shape of Circumferential Notch

Fig. 2 Configuration of Test Tubes

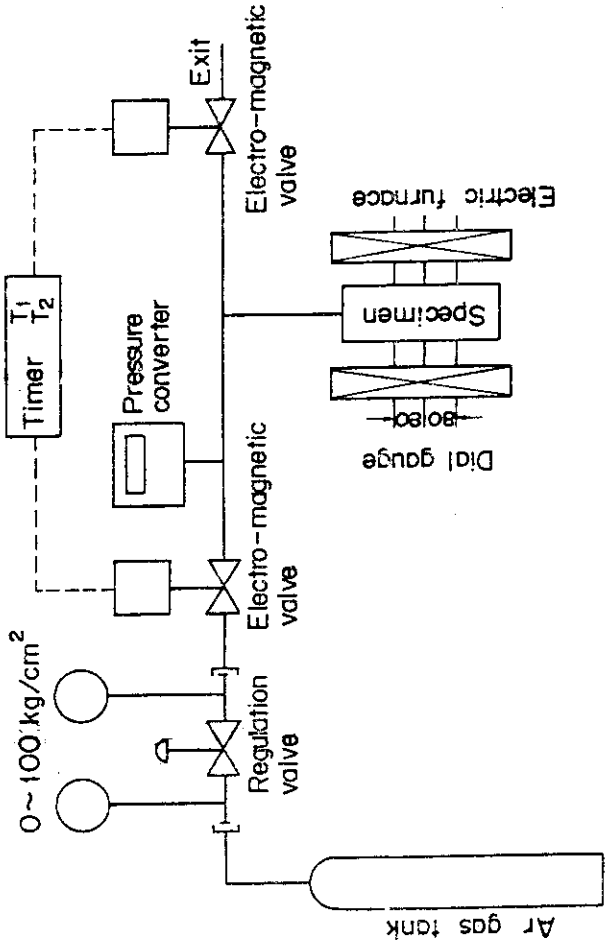

Fig. 1 Schematic of Test Equipment

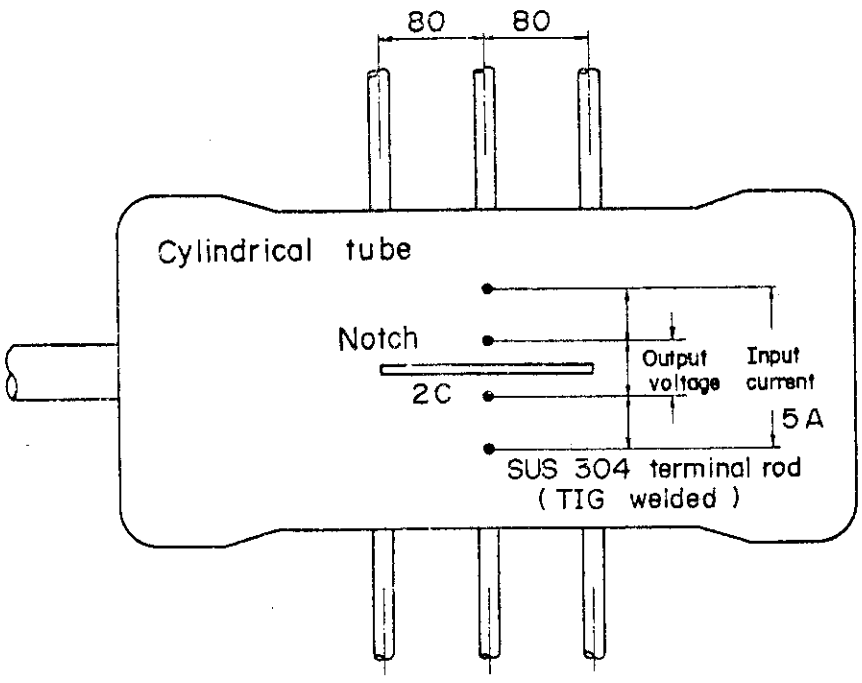

Rods for measuring creep deformation

Fig. 3 Arrangement of Electric Potential Probe

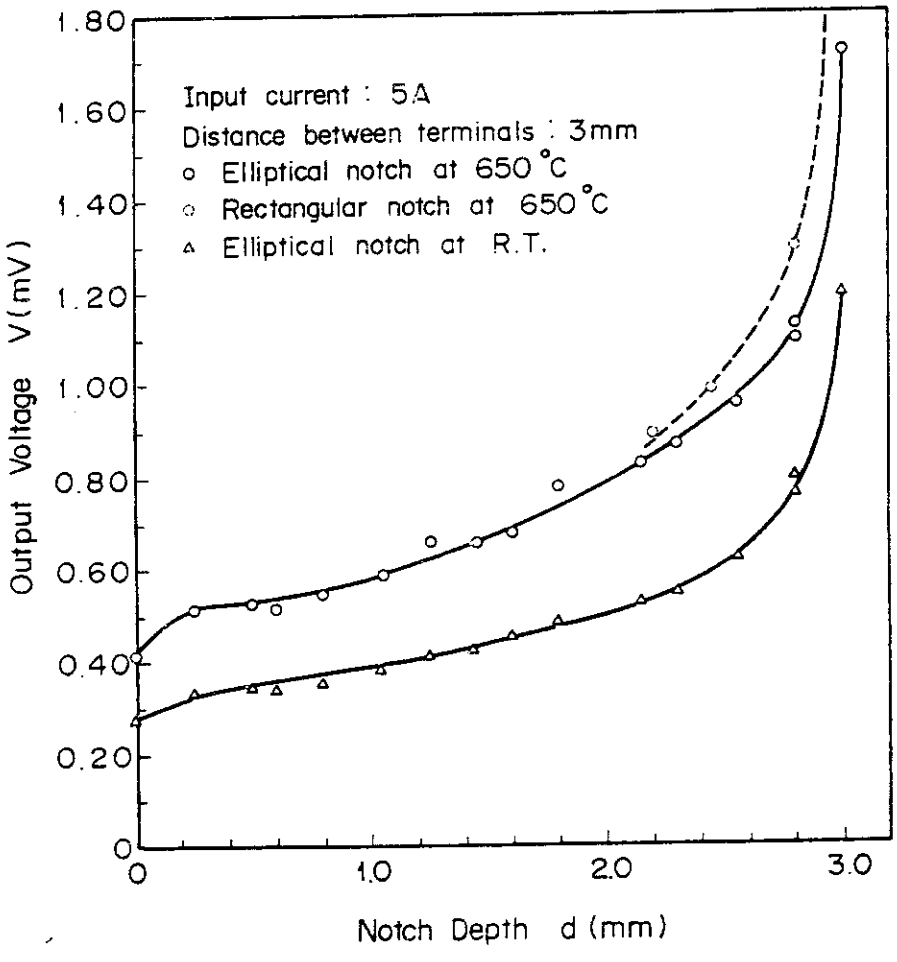

Fig. 4 Relation between notch depth and output voltage

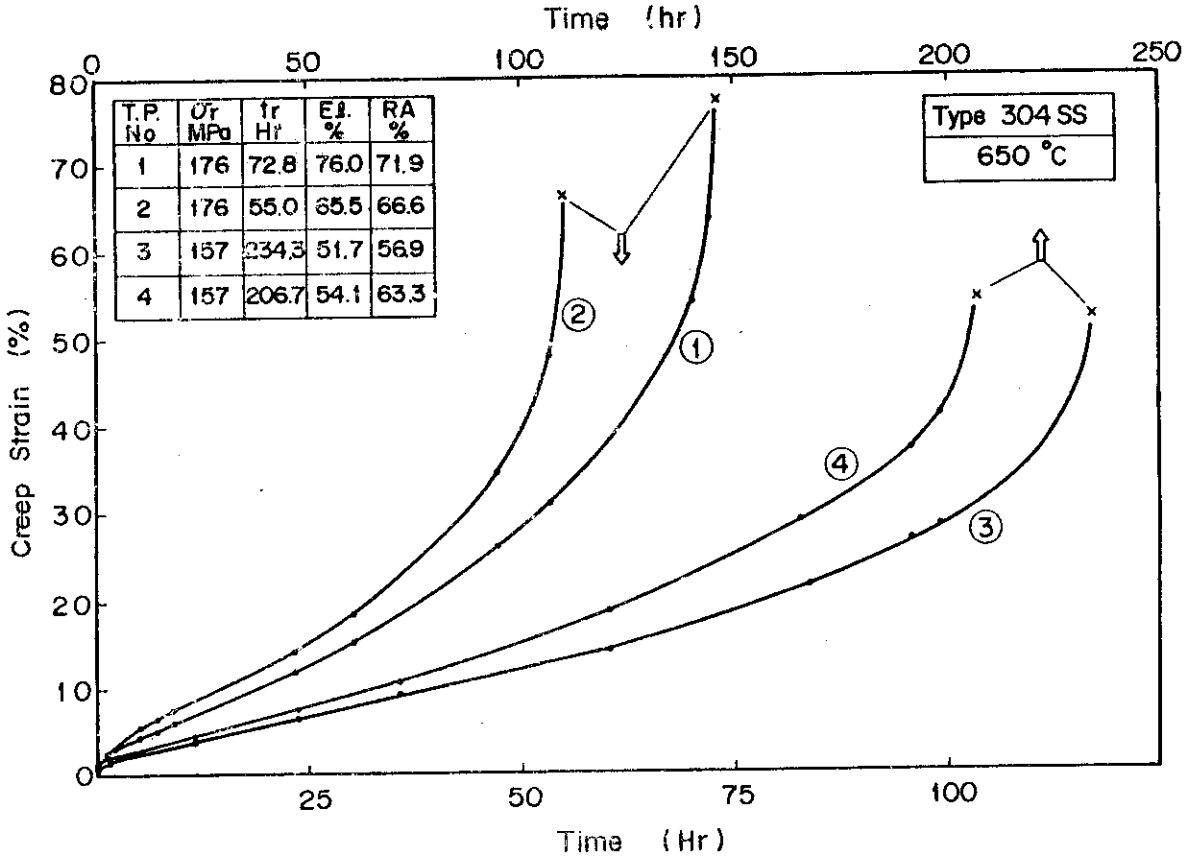

Fig. 5 Creep Deformation Behavior of Test Materials (I)

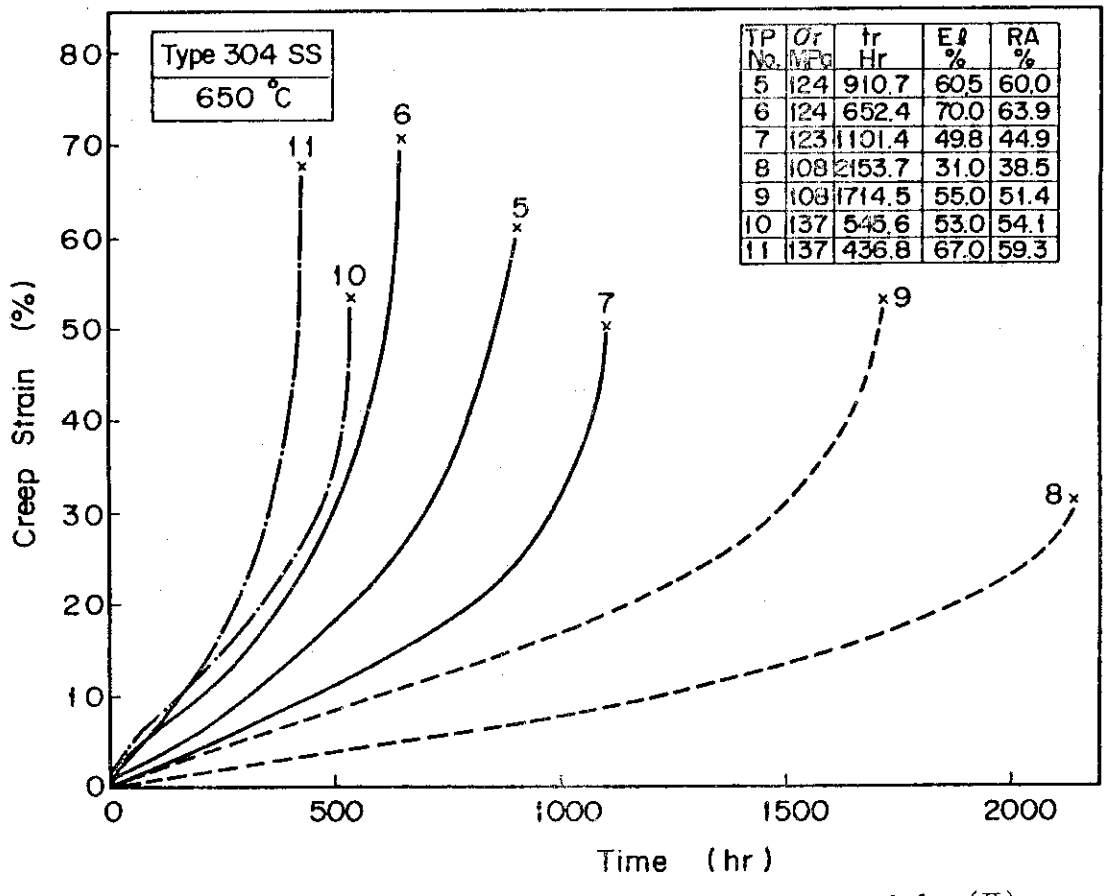

Fig. 6 Creep Deformation Behavior of Test Materials (II)

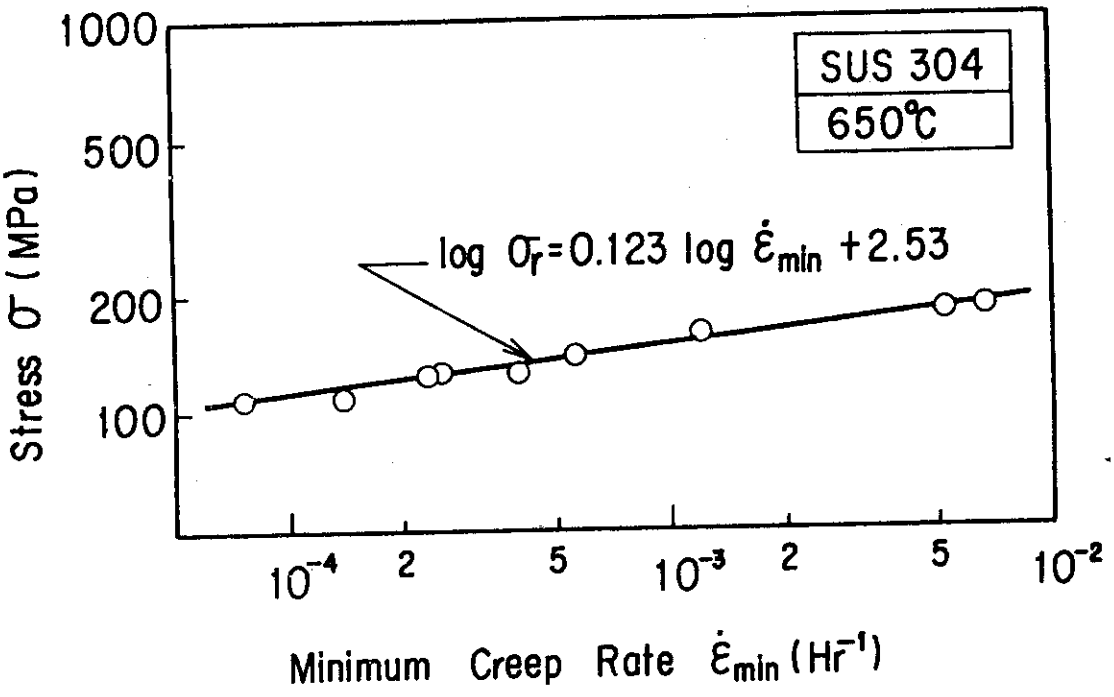

Fig. 7 Relation between Minimum Creep Rate and Stress

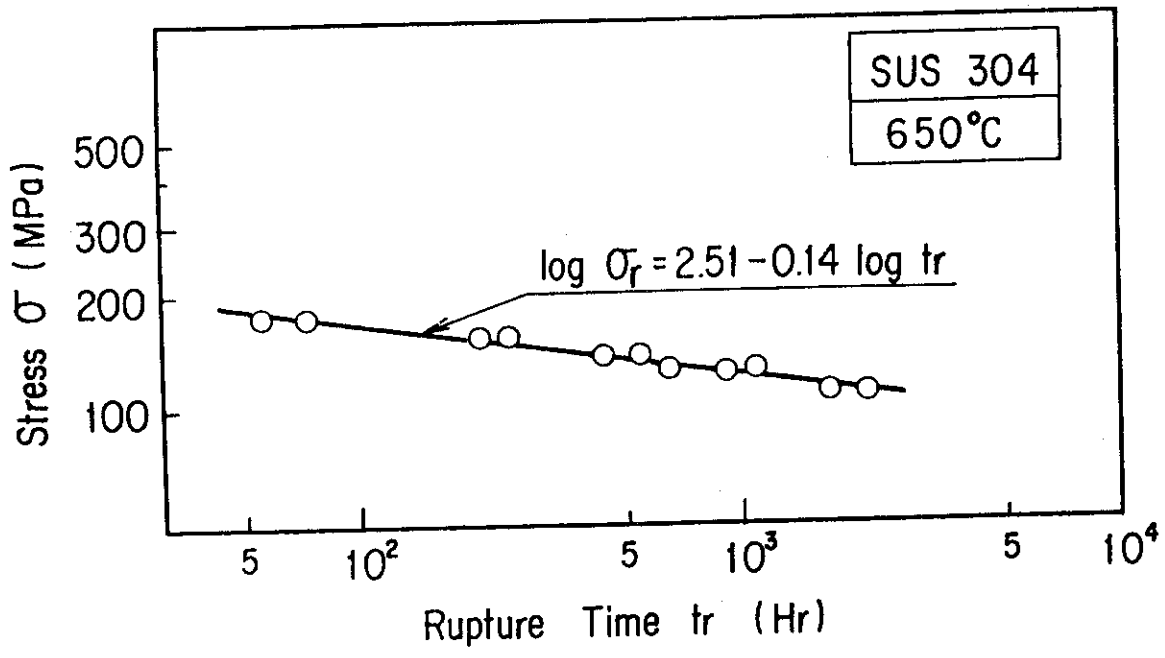

Fig. 8 Relation between Creep Rupture Time and Stress

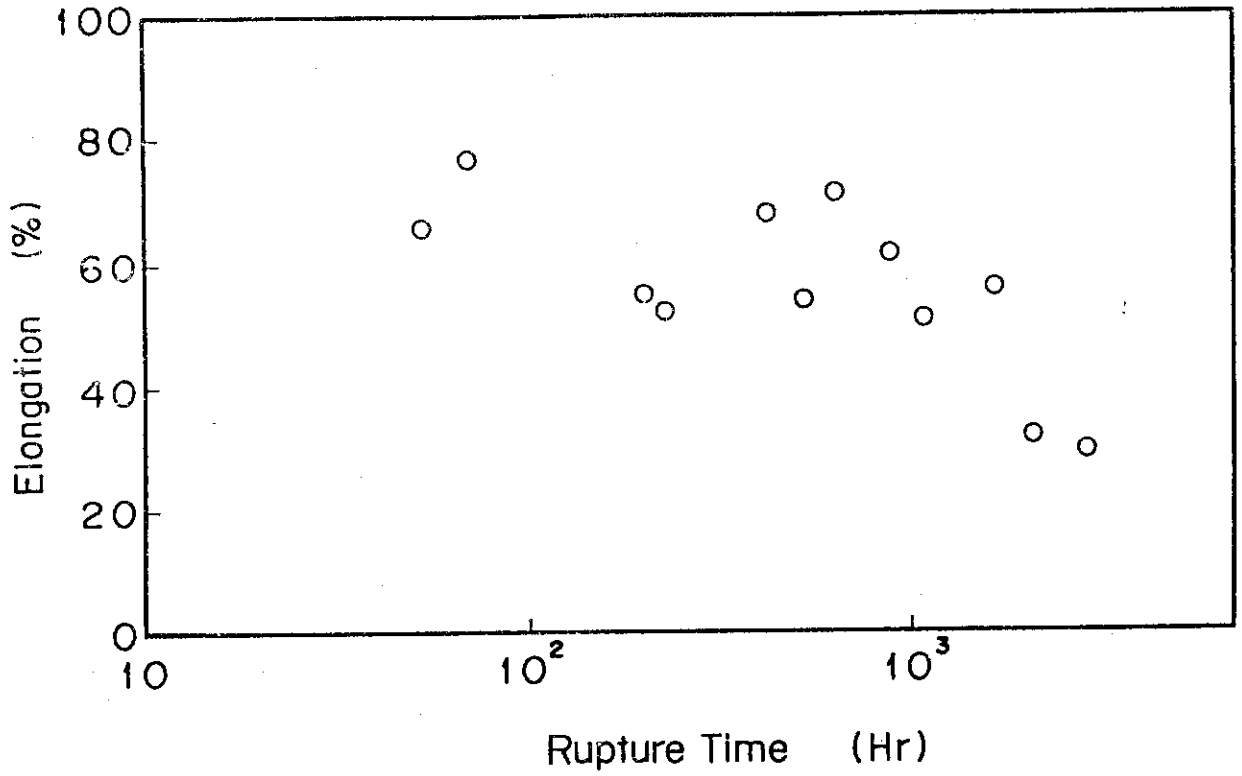

Fig. 9 Relation between Creep Elongation and Rupture Time

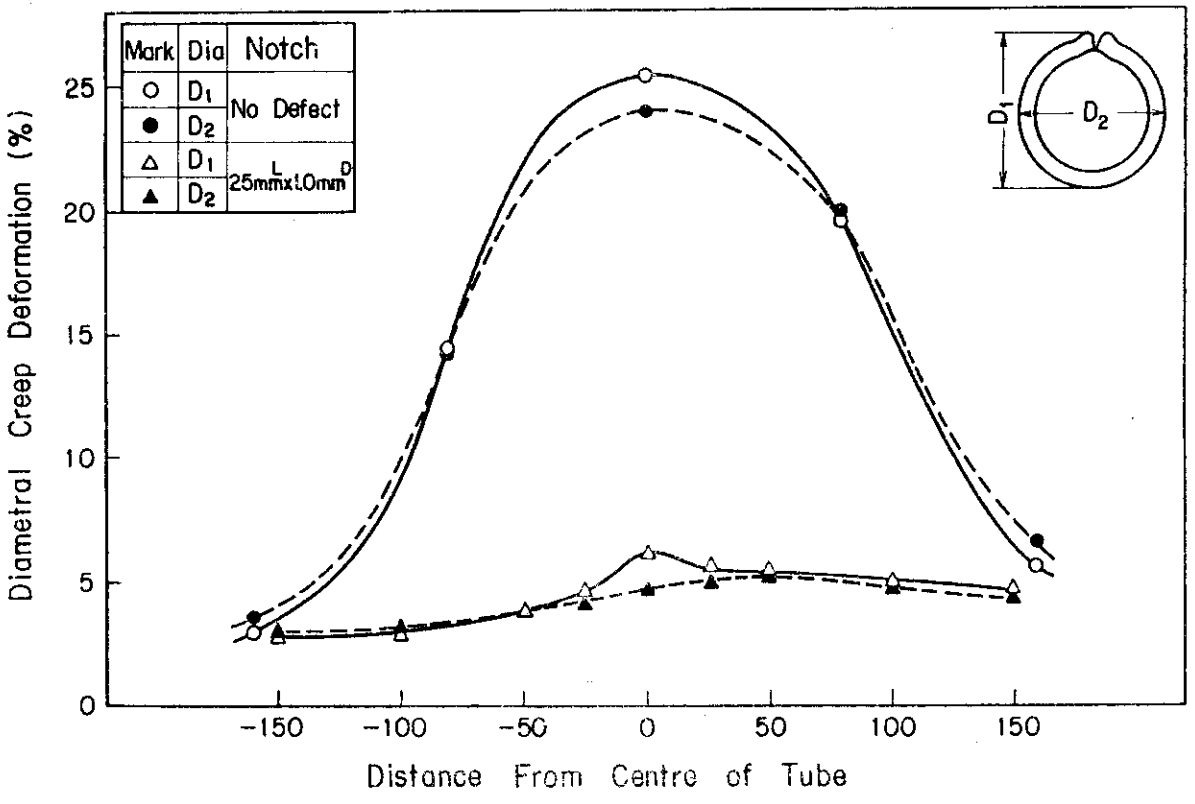

Fig.10 Distribution of Diametral Creep Deformation (Case of Axial Notch)

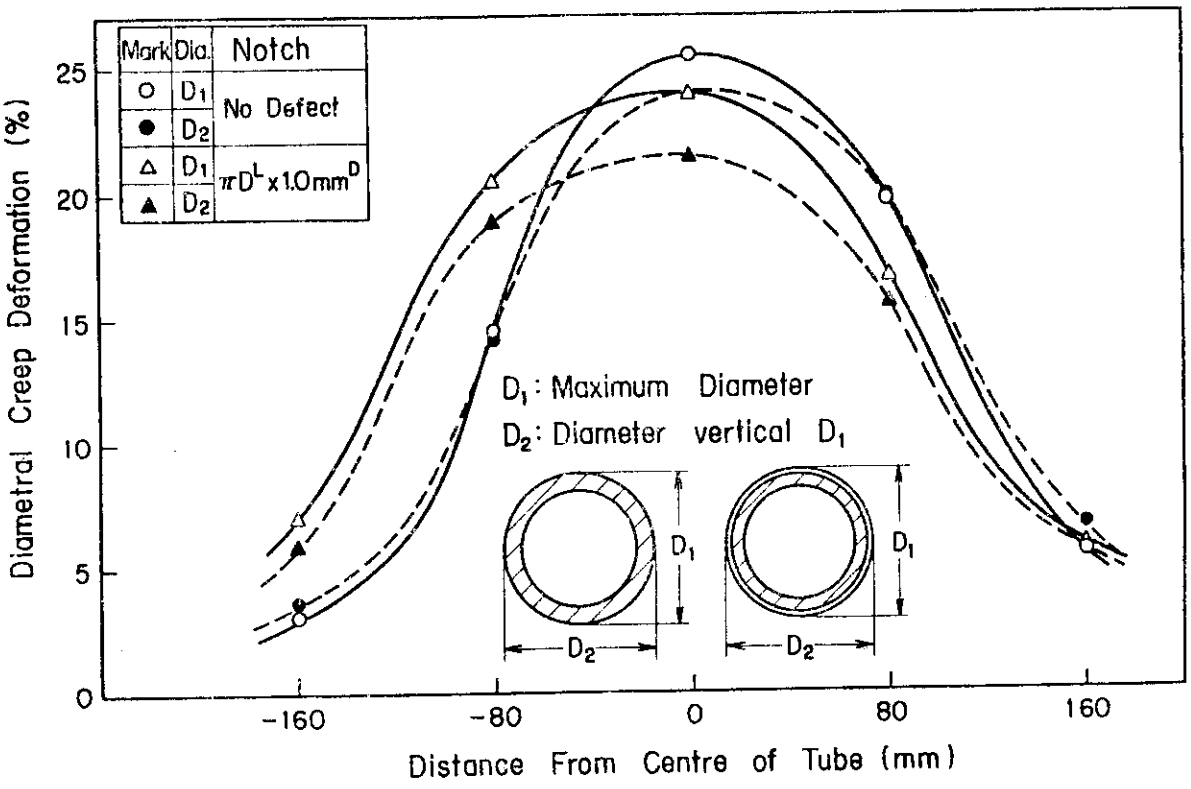

Fig.11 Distribution of Diametral Creep Deformation (Case of Circumferential Notch)

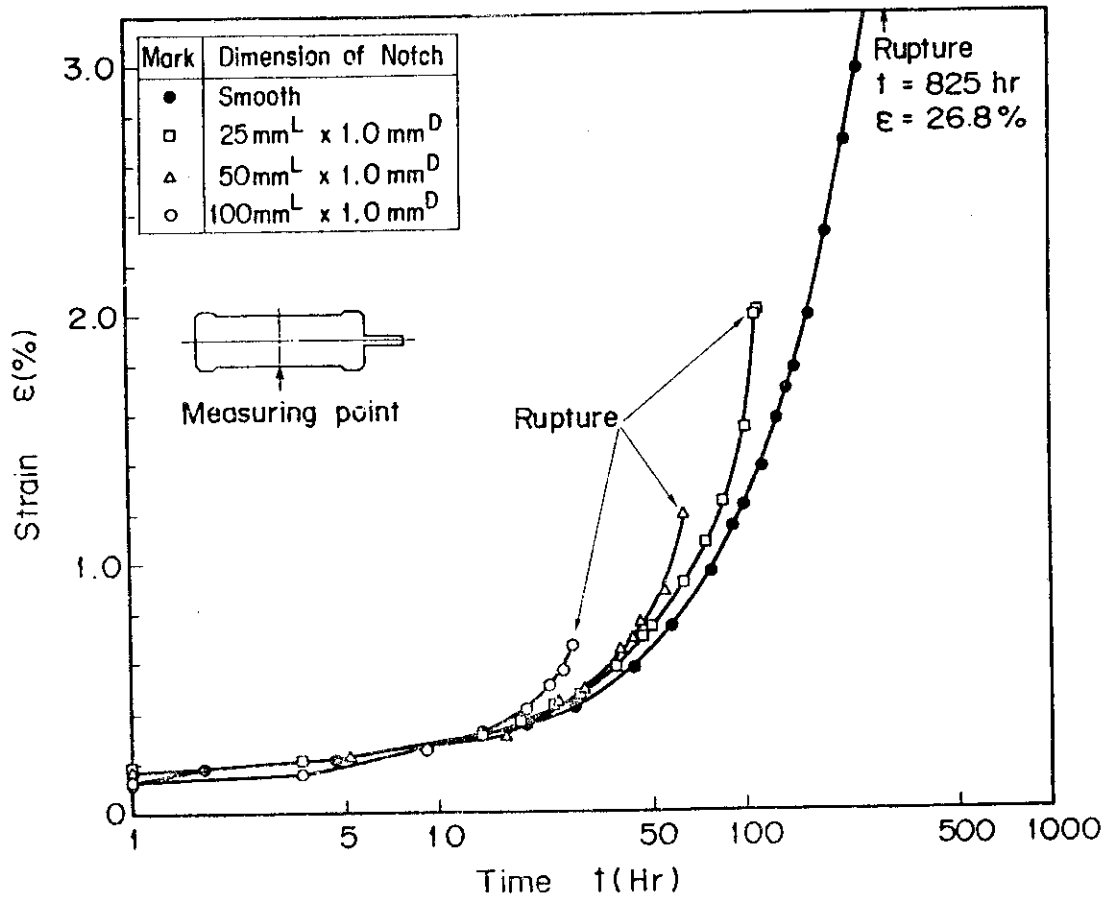

Fig.12 Creep Strain Versus Time of Tubes with and without Axial Notch

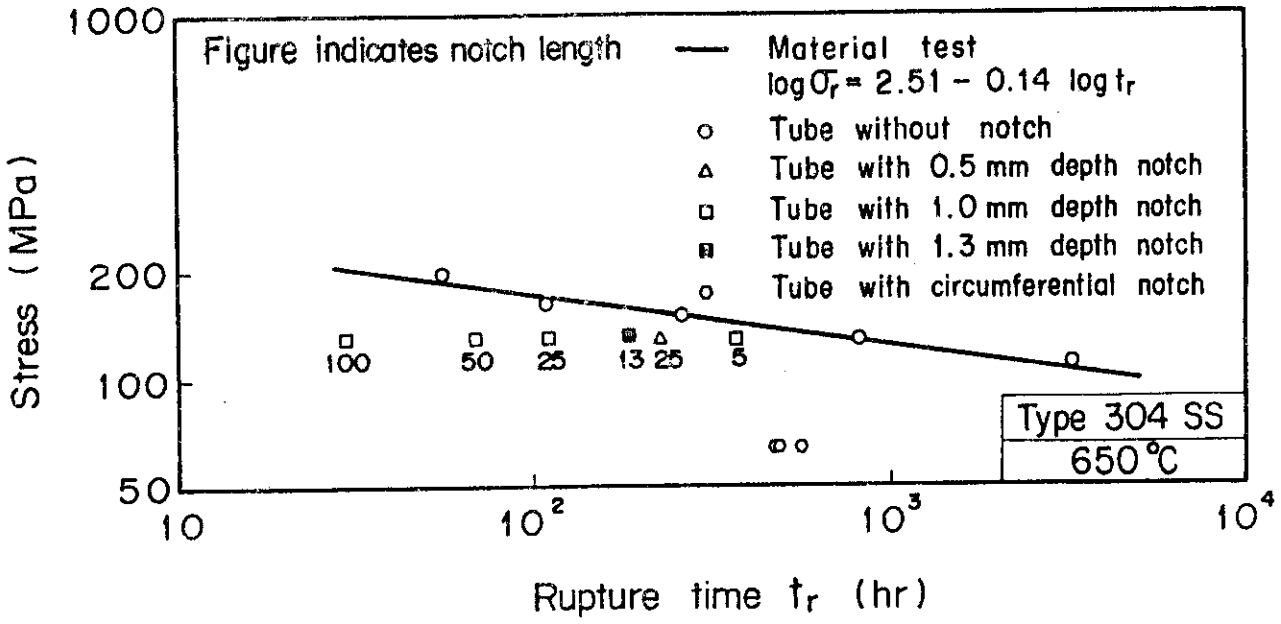

Fig.13 Relation between Nominal Stress of Tubes and Rupture Time

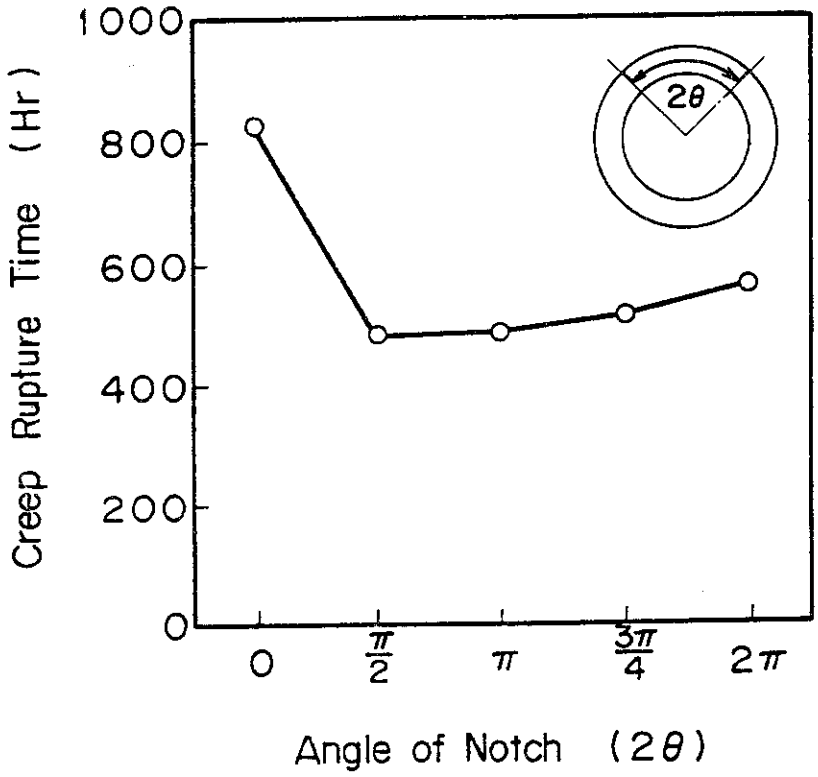

Fig.14 Creep Rupture Time versus Circumferential Notch Length

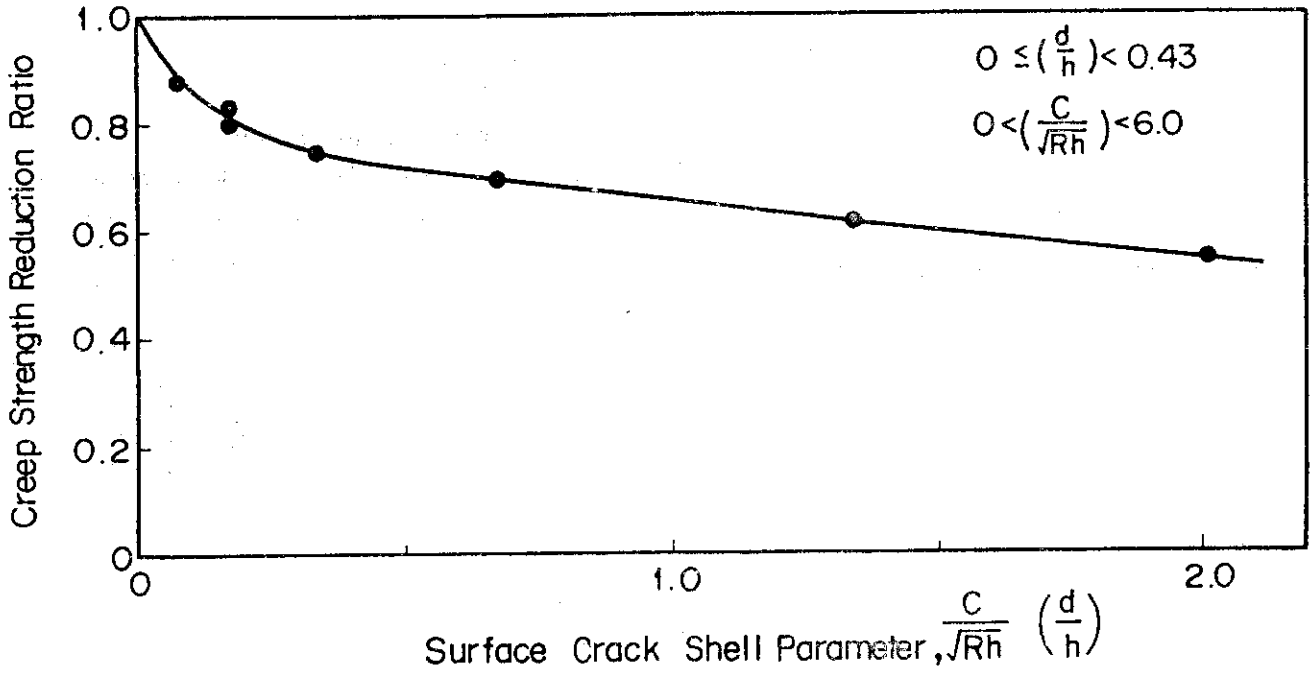

Fig.15 Relation between Creep Strength Reduction Ratio and Surface Shell Parameter

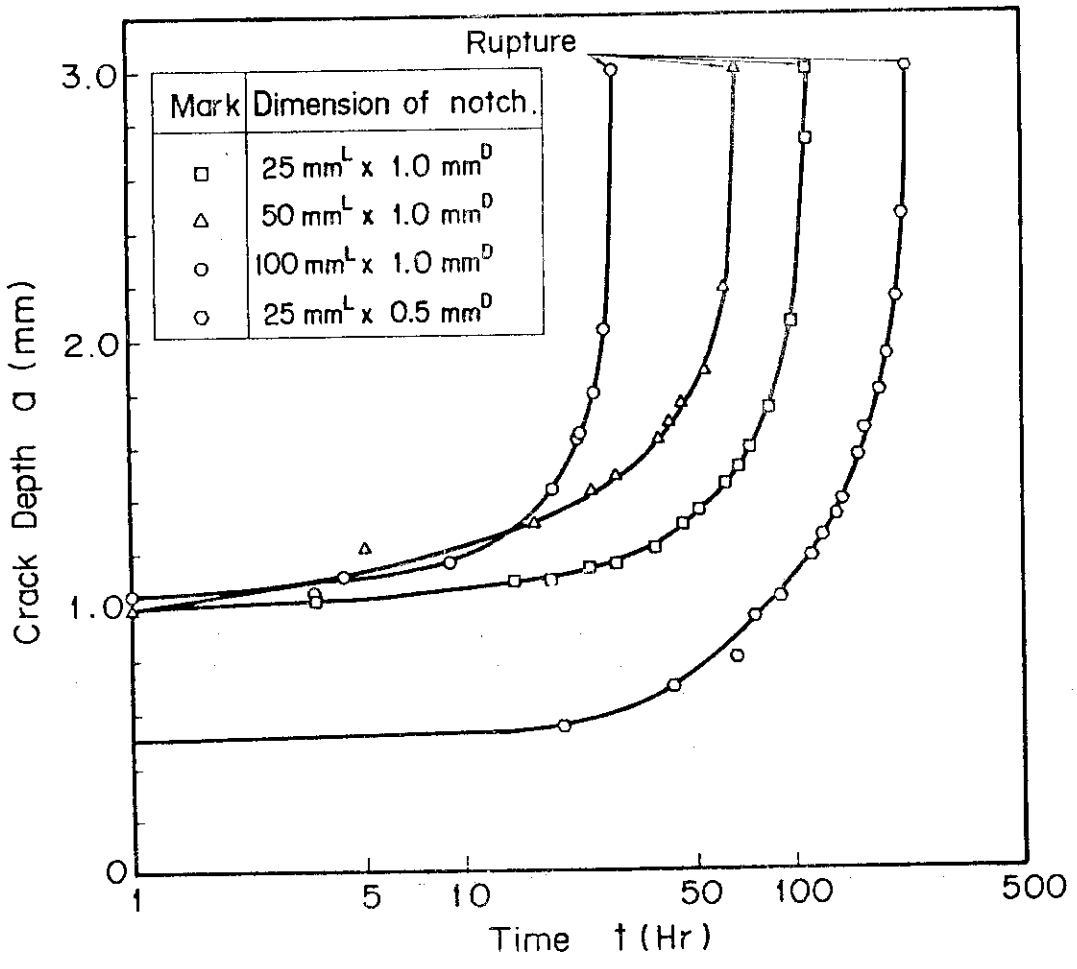

Fig.16 Creep Crack Growth Curve for Case of Axial Notch

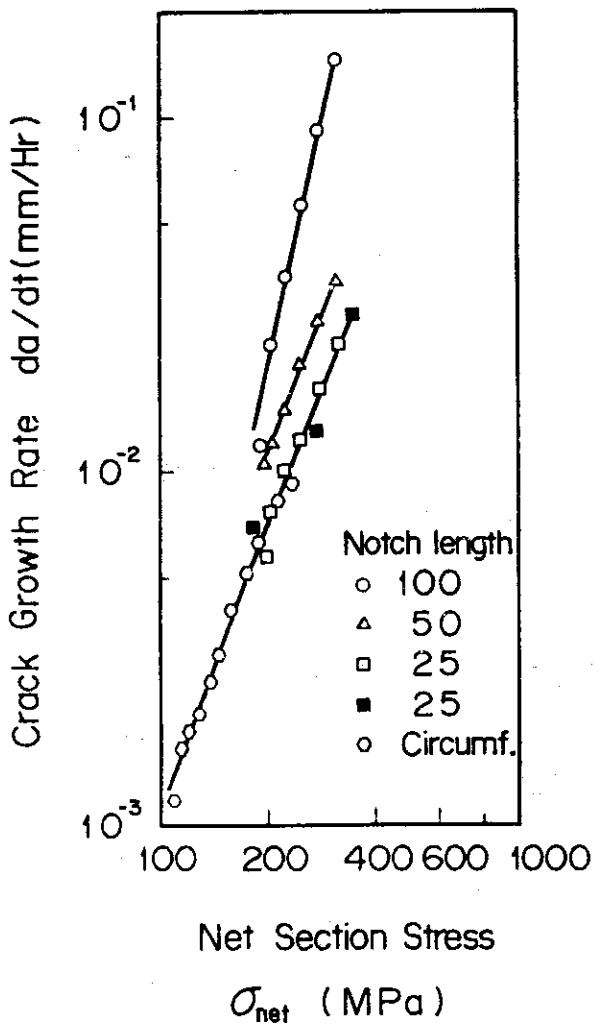

Fig.17 Relation between Creep Crack Growth Rate and Net Section Stress

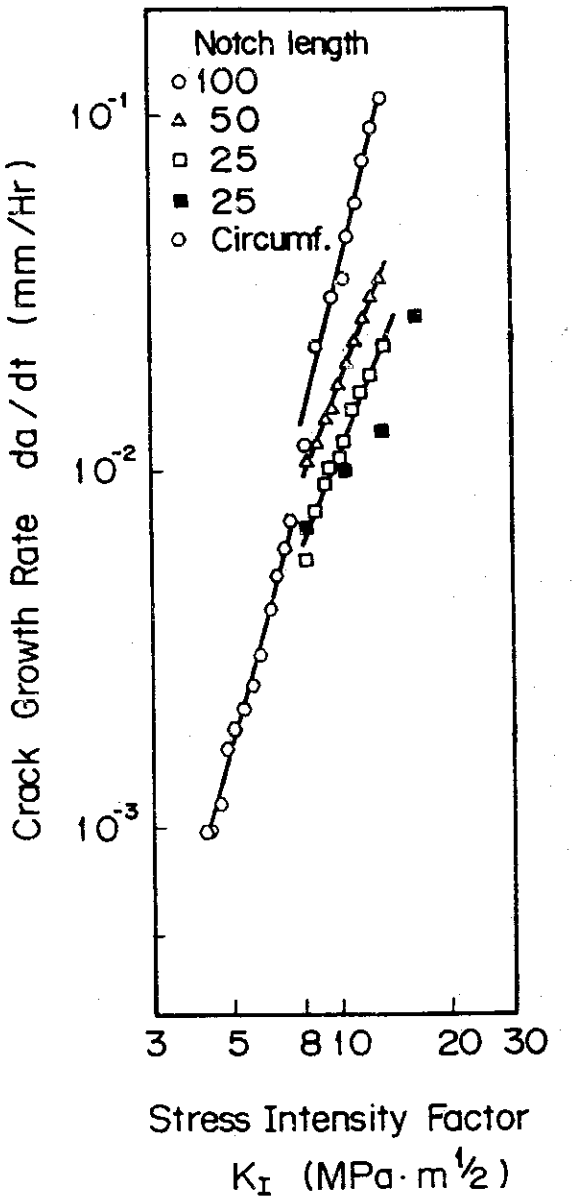

Fig.18 Relation between Creep Crack Growth Rate and Stress Intensity Factor

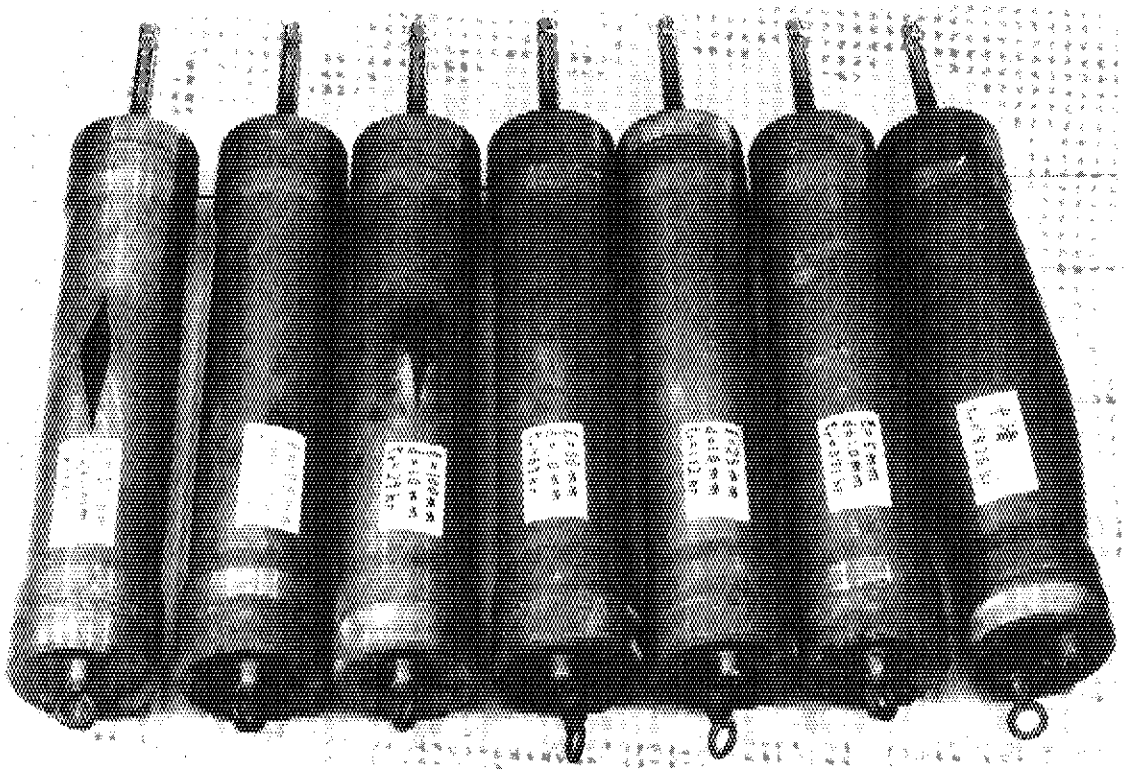

Fig.19 Fracture Apparance of Tubes Containing Axial Notch

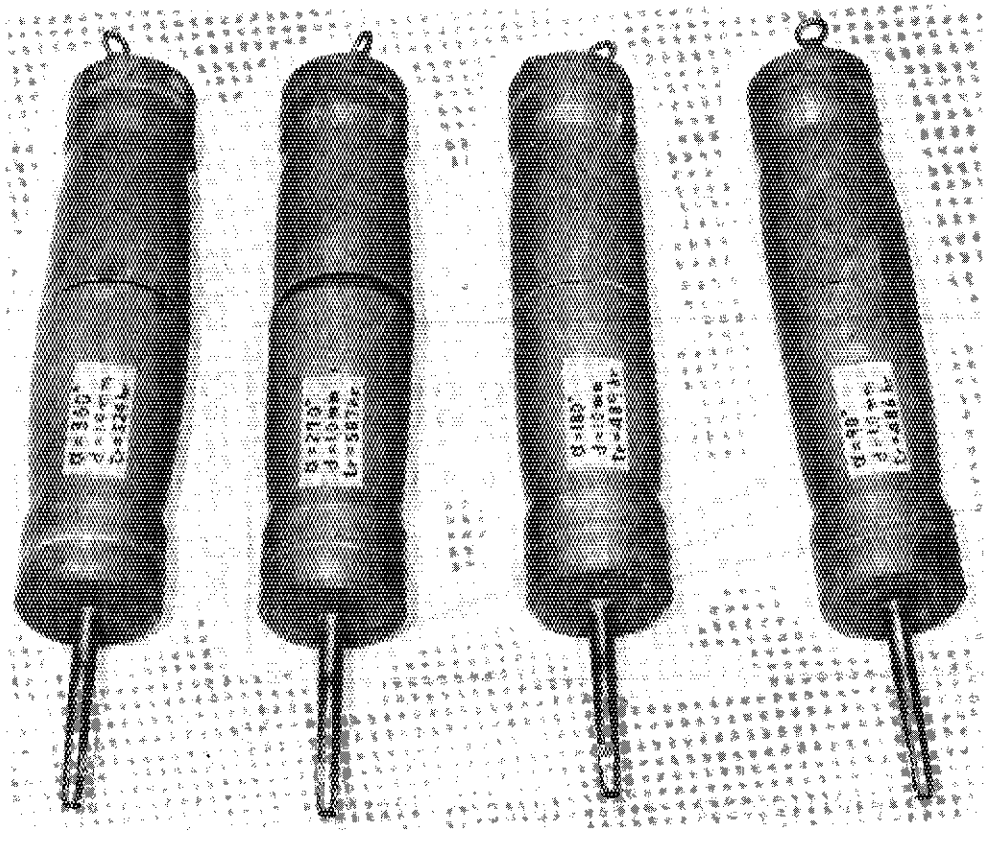

Fig.20 Fracture Appearance of Tubes Containing circumferential Notch